



A phenylacetaldehyde–flavonoid adduct, 8-*C*-(*E*-phenylethenyl)-norartocarpetin, exhibits intrinsic apoptosis and MAPK pathways-related anticancer potential on HepG2, SMMC-7721 and QGY-7703



Zong-Ping Zheng^a, Yan Yan^a, Ji Xia^b, Shuang Zhang^a, Mingfu Wang^c, Jie Chen^{a,d}, Yang Xu^{b,*}

^a State Key Laboratory of Food Science and Technology, Jiangnan University, Wuxi, Jiangsu, People's Republic of China

^b School of Pharmaceutical Sciences, Xiamen University, Xiamen, Fujian, People's Republic of China

^c School of Biological Sciences, The University of Hong Kong, Hong Kong, People's Republic of China

^d Synergetic Innovation Center of Food Safety and Nutrition, Jiangnan University, Wuxi, Jiangsu, People's Republic of China

ARTICLE INFO

Article history:

Received 31 July 2015

Received in revised form 5 November 2015

Accepted 19 November 2015

Available online 27 November 2015

Keywords:

Flavonoids

2-amino-1-methyl-6-phenylimidazo[4,5-*b*]pyridine (PhIP)

Phenylacetaldehyde

Flavonoid–phenylacetaldehyde adducts

Cytotoxicity effects

ABSTRACT

Norartocarpetin, quercetin and naringenin were found to effectively inhibit 2-amino-1-methyl-6-phenylimidazo[4,5-*b*]pyridine (PhIP) formation through trapping its phenylacetaldehyde and form their adducts in roast beef patties. Six adducts [8-*C*- or 6-*C*-(*E*-phenylethenyl) flavonoids] formed between phenylacetaldehyde and three flavonoids were detected in roast beef patties by UPLC–MS analyses and compared with their synthetic references. These flavonoid–phenylacetaldehyde adducts were synthesised and further subjected to cytotoxicity tests on three liver cancer cell lines HepG2, SMMC-7721 and QGY-7703. The adduct 8-*C*-(*E*-phenylethenyl)norartocarpetin (**NARA1**) was found to significantly induce cancer cell death with IC_{50} values about 7 μ M. After pre-treating with MAPK and caspase inhibitors, alteration of the cell morphology and cleaved-PARP were detected in liver cancer cell lines administered with **NARA1**. These data indicated that norartocarpetin could inhibit PhIP formation in roast beef patties and form norartocarpetin–phenylacetaldehyde adducts. The adduct **NARA1** has anticancer potential *via* intrinsic caspase-dependent and cell context-dependent MAPKs pathways.

© 2015 Elsevier Ltd. All rights reserved.

1. Introduction

2-Amino-1-methyl-6-phenylimidazo[4,5-*b*]pyridine (PhIP) is one of the most abundant heterocyclic amines (HAs) with mutagens found in food such as cooked meat and fish products (Murkovic, Weber, Geiszler, Fröhlich, & Pfannhauser, 1999; Skog, Johansson, & Jagerstad, 1998; Wakabayashi, Nagao, Esumi, & Sugimura, 1992; Warzecha et al., 2004). Various studies have demonstrated that high intakes of food containing heterocyclic amines enhance the risk of cancer development in liver, mammary gland, colon, and prostate (Ambrosone, Abrams, Gorlewska-Roberts, & Kadlubar, 2007; Malfatti et al., 2006; Tang et al.,

2007). Recent studies also suggest that there is a positive correlation between red meat consumption, PhIP intake, and some cancers (Bogen et al., 2007; Shin et al., 2007; Sinha et al., 2000, 2005). In order to reduce the intake of heterocyclic amines, many strategies have been proposed to minimise heterocyclic amine formation, such as avoiding prolonged heat treatment at high temperature, marinating meat with certain natural ingredients before cooking (Ahn & Grun, 2005; Busquets, Puignou, Galceran, & Skog, 2006; Murkovic, Steinberger, & Pfannhauser, 1998; Skog, Steineck, Augustsson, & Margaretha, 1995). Recently, Cheng et al. (2008, 2009) confirmed that some flavonoids, such as naringenin and epigallocatechin gallate (EGCG), could seriously reduce the level of PhIP in model systems and real meat samples. The study of Salazar, Arambula-Villa, Hidalgo, and Zamora (2014) also showed that some phenols were efficient inhibitors of PhIP formation. Both studies showed that some phenolics could effectively inhibit PhIP formation in food or model systems.

Phenylacetaldehyde, a volatile compound from the degradation of phenylalanine, is present in some foods and flowers (Chu & Yaylayan, 2008; Tieman, Loucas, Kim, Clark, & Klee, 2007). Previous studies have shown that the precursors of creati(ni)ne,

Abbreviations: PhIP, 2-amino-1-methyl-6-phenylimidazo[4,5-*b*]pyridine; HA, heterocyclic amine; EGCG, epigallocatechin gallate; NA1, 8-*C*-(*E*-phenylethenyl) naringenin; NA2, 6-*C*-(*E*-phenylethenyl)naringenin; NARA1, 8-*C*-(*E*-phenylethenyl) norartocarpetin; NARA2, 6-*C*-(*E*-phenylethenyl)norartocarpetin; QA1, 8-*C*-(*E*-phenylethenyl)quercetin; QA2, 6-*C*-(*E*-phenylethenyl)quercetin; COX-1, cyclooxygenase-1; UPLC, ultra-performance liquid chromatography; MTT, 3-(4,5-dimethylthiazol-2-yl)-2,5-diphenyl tetrazolium bromide.

* Corresponding author.

E-mail address: xu_yang@xmu.edu.cn (Y. Xu).

phenylacetaldehyde, ammonia and formaldehyde participate in the formation of PhIP. Phenylacetaldehyde plays a key role in PhIP formation (Murkovic et al., 1999; Zamora, Alcon, & Hidalgo, 2014). Reducing the level of phenylacetaldehyde in food will therefore inhibit PhIP formation. Cheng et al. (2008, 2009) have further proved that scavenging of phenylacetaldehyde could greatly reduce the level of PhIP in model systems and real meat samples, and the possible mechanism was that these flavonoids trapped phenylacetaldehyde to form their interaction adducts. However, the toxicity and biological activity of these adducts are unreported so far. The recent finding of Li et al. (2014) showed that 6-C-(*E*-phenylethenyl)naringenin could potently suppress the anchorage independent growth by inhibiting COX-1 activity and effectively inhibiting tumour growth in a 28-day colon cancer xenograft model without any obvious systemic toxicity. The finding is very meaningful because it showed that some flavonoids not only can inhibit the formation of some hazardous substances (for example PhIP) but also convert them into new adducts with anticancer potential through trapping these hazardous substances or their intermediates during food processing.

PhIP can induce chromosomal aberrations and sister-chromatid exchanges to form PhIP–DNA adducts and lead to PhIP-induced carcinogenesis, and high doses of HAs can cause liver tumours (Bacon et al., 2003; Freedman et al., 2010). The inhibition of PhIP formation through decreasing the content of final products or trapping its intermediate products in meat will greatly reduce the risk of carcinogenesis.

The aim of the present study was to unravel the inhibitory abilities of three flavonoids (naringenin, quercetin and norartocarpetin) on the formation of PhIP in roast beef patties, and to investigate the cytotoxicity activities of six flavonoid–phenylacetaldehyde adducts on liver cancer cell lines, including HepG2, SMMC-7721, and QGY-7703.

2. Materials and methods

2.1. Chemicals

Phenylacetaldehyde was purchased from Sigma–Aldrich Co. (St. Louis, MO). All solvents used were of analytical grade and were purchased from Sinopharm Chemical Reagent Co, Ltd. (Shanghai, P. R. China). Methanol (MeOH) and acetonitrile were purchased from J&K Scientific (Beijing, P. R. China). Naringenin and quercetin were purchased from Nanjing Ze Lang Medical Technology CO, Ltd. (P. R. China). Norartocarpetin was isolated from the wood of *Artocarpus heterophyllus* in our previous studies (Zheng et al., 2014). PhIP was purchased from Toronto Research Chemicals Inc. (Toronto, Canada). Oasis MCX cartridges (3 mL/60 mg) were purchased from Waters (Milford, MA). Sephadex LH-20 was from GE Healthcare Bio-Sciences AB (Uppsala, Sweden). The primary antibodies for PARP and caspase-9 were brought from Cell Signaling (Beverly, MA). Anti- β -actin was from Sigma. Anti-mouse and rabbit secondary antibodies were purchased from Thermo.

2.2. Effect of flavonoids on the PhIP formation in roast beef patties

Fresh ground beef was purchased from the local supermarket. The ground beef (40 g) was thoroughly mixed with different flavonoid powder (0.2 mM), and then moulded into beef patties using a Petri dish (6 × 1.5 cm). The beef patties were roasted in an electric oven for 20 min (10 min per side) at 230 °C and homogenised after cooling.

A method was used for the extraction of PhIP described by Messner and Murkovic (2004). Roast beef (5 g) was dissolved into 30 mL 1 M sodium hydroxide (NaOH) and homogenised for 2 min.

After that, the viscous solution was mixed with diatomaceous earth and poured into empty Extrelut[®] columns (Millipore, Billerica, MA) with ethyl acetate as the eluent. The concentrated eluate was then transferred into Oasis MCX cartridges (Waters) activated with 6 mL MeOH, 6 mL water and then 6 mL ethyl acetate. The cartridges were washed with 6 mL 0.1 M hydrochloric acid (HCl) and 6 mL MeOH twice, respectively. The analytes were eluted with 6 mL of MeOH:aqueous ammonia mixture (19:1). The analytes were concentrated under nitrogen flushing and dissolved in 500 μ L MeOH and then subjected to UPLC–MS analysis.

2.3. UPLC–MS analysis of PhIP in roast beef patties

PhIP was analysed on a Waters UPLC with tandem mass spectrometry according to our previous study (Yan et al., 2014). Separation was carried out on an Acquity BEH C18 column (1.7 μ m; 50 × 2.1 mm I.D.; Waters), with 10 mM ammonium acetate (solvent A) and acetonitrile (solvent B) with the following gradients: 0 min 90% A; 0.1 min 90% A; 18 min 70% A; 20 min 100% B; 20.1 min 90% A; total flow was 0.3 mL/min. The injection volume was 1 μ L. The MS conditions were as follows: positive ion mode; spray voltage, 2.8 V; ion source temperature, 120 °C; desolvation temperature, 350 °C.

2.4. Extraction and detection of flavonoid–phenylacetaldehyde adducts in roast beef patties

Roast beef (20 g) was mixed with MilliQ water (50 mL) and homogenised for 5 min. After that, the cloudy suspensions were extracted twice with ethyl acetate (200 mL). The concentrated eluate was then evaporated to dryness and defatted by adding 2 mL methanol and stored at –20 °C. Subsequently, the methanol mixture was centrifuged to remove the precipitated fat, and was filtered before being analysed on a Waters UPLC–Q–TOF system.

2.5. UPLC–MS analysis of flavonoid–phenylacetaldehyde adducts

Phenylacetaldehyde–flavonoid adducts were detected on a Waters UPLC–Q–TOF system, equipped with a SYNAPT mass spectrometer and a Waters Acquity UPLC. Separation was carried out on an Acquity BEH C₁₈ column (50 mm × 2.1 mm, 1.7 μ m). The mobile phase composed of water containing 0.1% formic acid (solvent A) and methanol (solvent B). Gradient elution was as follows: 0 min, 95% A; 0.1 min, 95% A; 6 min, 40% A; 8 min, 100% B; 9 min, 100% B; 9.1 min, 95% A; 12 min, 95% A. The MS conditions were as follows: negative ion mode, spray voltage 2.8 V, cone voltage 31 V, source temperature 110 °C, desolvation temperature 400 °C, scan range 100–1500 Da.

2.6. High performance liquid chromatography (HPLC) used to detect the pure adducts

HPLC analysis was performed on a Shimadzu HPLC system equipped with a separation module (LC-20AT), an autosampler (SIL-20A), a degasser (DGU-20A3), a photodiode array detector (SPD-M20A) and a reverse-phase GraceSmart column (4.6 μ m, 2.1 × 250 mm, Ryss Tech Ltd., Shanghai, P. R. China). With mobile phases of 0.1% formic acid in water (solvent A) and acetonitrile (B) the following program was used: 0 min, 95% A; 35 min, 20% A; 37 min, 95% A; 50 min 95% A.

2.7. Synthesis of flavonoid–phenylacetaldehyde adducts

Sample preparation was according to the previous method (Cheng et al., 2008) and slightly modified. Firstly, phenylacetaldehyde solution was prepared by adding 280 μ L phenylacetaldehyde

into 42.72 mL di(ethylene) glycol. Secondly, 1 mM flavonoid (naringenin, norartocarpetin, quercetin) was added into the prepared 43 mL phenylacetaldehyde solution, and then the mixture was vortexed and sonicated until all the flavonoid was dissolved. Thirdly, 1 mL 37% HCl was added into 6 mL Milli-Q water to prepare 7.0 mL 5.3% HCl solution. Finally, 7 mL 5.3% HCl solution was then added into the phenylacetaldehyde solution. The reaction mixture was heated at 130 °C for 2 h, and then the reaction mixture was inserted in an ice-water bath. After cooling, the reaction solution (50 mL) was transferred into a separating funnel; 50 mL Milli-Q water and 100 mL ethyl acetate were added into the funnel. The solution was shaken vigorously and left to separate, and the clear supernatant was collected. The above extraction process was repeated for another two times. The clear supernatant from three repeated extraction processes was pooled and concentrated on a rotary evaporator under vacuum.

2.8. Isolation and characterisation of flavonoid–phenylacetaldehyde adducts

The above reaction products were isolated by column chromatography and the structures of flavonoid–phenylacetaldehyde adducts were determined by NMR spectroscopy on 300 and 400 MHz spectrometers (Bruker) and ESI-MS data.

2.8.1. Naringenin–phenylacetaldehyde adducts

The extract obtained is re-dissolved in methanol and then loaded onto a Sephadex LH-20 column (80 × 2 cm). Elution was performed with 80% methanol in water; the flow was set at 10 mL/15 min (the volume of one tube), and the chromatographic fractions were collected with an automatic fraction collector. The collected fractions were firstly assessed by thin layer chromatography (TLC) to detect adducts and then were confirmed by HPLC to ensure the purity of isolated compound up to 95% (relative peak area, estimated). The pure fractions were combined and further isolated by the same method until the two isomers of the adducts were separated. Two adducts of 8-*C*-(*E*-phenylethenyl)naringenin (**NA1**, 12.2 mg) and 6-*C*-(*E*-phenylethenyl)naringenin (**NA2**, 9.4 mg) were obtained in the end.

2.8.2. Norartocarpetin–phenylacetaldehyde adducts

The extract obtained is re-dissolved in methanol and then loaded onto a Sephadex LH-20 column. The following method is similar to the isolation procedure of naringenin–phenylacetaldehyde adducts. Elution is performed with 80% methanol (MeOH–H₂O) to offer 8-*C*-(*E*-phenylethenyl)norartocarpetin (**NARA1**, 8.4 mg) and 6-*C*-(*E*-phenylethenyl)norartocarpetin (**NARA2**, 6.8 mg).

2.8.3. Quercetin–phenylacetaldehyde adducts

The extract obtained is re-dissolved in methanol and then loaded onto a Sephadex LH-20 column. The following method is similar to the isolation procedure of naringenin–phenylacetaldehyde adducts. Elution is performed with 80% methanol in water to offer 8-*C*-(*E*-phenylethenyl)quercetin (**QA1**, 15.4 mg) and 6-*C*-(*E*-phenylethenyl)quercetin (**QA2**, 8.3 mg).

2.8.3.1. NA1 and NA2. Yellow powder; ESI-MS: m/z 373.1 [M–H][–], **NA1**: HR-ESI-MS: m/z 373.0992 [M–H][–] (calcd. 373.0998 for C₂₃H₁₇O₅), **NA2**: HR-ESI-MS: m/z 373.0998 [M–H][–] (calcd. 373.0998 for C₂₃H₁₇O₅); ¹H NMR and ¹³C NMR data are shown in Table S1.

2.8.3.2. NARA1 and NARA2. Yellow powder; ESI-MS: m/z 387.1 [M–H][–], **NARA1**: HR-ESI-MS: m/z 387.0811 [M–H][–] (calcd. 387.0869 for C₂₃H₁₅O₆), **NARA2**: HR-ESI-MS: m/z 387.0843

[M–H][–] (calcd. 387.0869 for C₂₃H₁₅O₆); ¹H NMR and ¹³C NMR data are shown in Table 1.

2.8.3.3. QA1 and QA2. Yellow powder; ESI-MS: m/z 403.1 [M–H][–], **QA1**: HR-ESI-MS: m/z 403.0769 [M–H][–] (calcd. 403.0740 for C₂₃H₁₅O₇), **QA2**: HR-ESI-MS: m/z 403.0742 [M–H][–] (calcd. for 403.0740 C₂₃H₁₅O₇); ¹H NMR and ¹³C NMR data are shown in Table 1.

2.9. Cell culture and drug treatment

HepG2, SMMC-7721 and QGY-7703 cells were cultured in Dulbecco's Modified Eagle Medium (high glucose) and RPMI-1640, respectively, with 10% foetal bovine serum under standard culture conditions. When the cells grew to about 80% confluence, they were sub-cultured or treated with adducts. To determine whether chemicals induced cancer cell apoptosis through caspase-dependent pathways, the spectrum caspase inhibitor 50 μM broad Z-VAD-fmk was applied for 1 h before adduct treatments. To ascertain whether adducts induced cancer cell apoptosis via MAPK (p38, JNK, ERK) and PI3K pathways, their inhibitors were pretreated 1 h before adduct administrations, including 20 μM SB203580, 20 μM SP600125, 20 μM PD98059, and 20 μM LY294002.

2.10. DAPI staining analysis of cell apoptosis

Morphological changes of apoptosis were detected by fluorescence microscopy after staining with 1 μg/mL DAPI. All experiments were repeated three times and the representative pictures were exhibited.

2.11. Measurement of cell growth inhibition

The growth of cells was evaluated through 3-(4,5-dimethylthiazol-2-yl)-2,5-diphenyl tetrazolium bromide (MTT) assay. Cells were planted in 96-well microplates in 200 μL (5 × 10³/well). After 24 h, the cells were treated with FBS-free medium containing compounds (10, 20, and 40 μM) for 24 h. At the end of the experiments, 20 μL of 5 μg/mL MTT were added to each well. Cells were then incubated at 37 °C for 4 h. Formazan was solubilised by 100 μL DMSO and measured at 570 nm. All experiments were repeated three times. The 50% inhibiting concentration (IC₅₀) was recorded as mean ± SD (μM).

2.12. Western blot analysis

Western blot analysis was performed as previously described (Zheng et al., 2014). Equal amounts of protein were separated by SDS–PAGE. After they were transferred onto membranes, the proteins were probed with corresponding antibodies and detected by ECL detection reagents (GE Healthcare).

2.13. Statistical analysis

Results are expressed as the mean ± SD. Statistical analysis was done by using a two-tailed Student's *t* test; *p* < 0.05 was considered as significant.

3. Results and discussion

3.1. Effect of flavonoids on PhIP formation in roast beef patties

Fruits, vegetables, and spices are rich in flavonoids, and they play an important role in human health. In this study, naringenin, norartocarpetin, and quercetin were evaluated for their effects on

Table 1
¹H NMR and ¹³C NMR data of four new flavonoid–phenylacetaldehyde adducts (DMSO-*d*₆, J in Hz).

No.	NARA1		NARA2		QA1		QA2	
	¹ H NMR ^a	¹³ C NMR ^b	¹ H NMR ^a	¹³ C NMR ^b	¹ H NMR ^a	¹³ C NMR ^b	¹ H NMR ^c	¹³ C NMR ^d
2		161.8 (C)		159.6 (C)		147.4 (C)		146.9 (C)
3	6.95 (1H, s)	107.9 (CH)	7.02 (1H, s)	108.5 (CH)		135.8 (C)		135.7 (C)
4		182.0 (C=O)		182.0 (C=O)		176.0 (C=O)		176.0 (C=O)
5		158.8 (C)		158.9 (C)		153.5 (C)		154.4 (C)
6	6.34 (1H, s)	98.6 (CH)		107.8 (C)	6.37 (1H, s)	98.3 (CH)		107.3 (C)
7		162.4 (C)		161.8 (C)		162.6 (C)		161.9 (C)
8		104.0 (C)	6.58 (1H, s)	93.5 (CH)		103.6 (C)	6.56 (1H, s)	93.1 (CH)
9		160.2 (C)		161.6 (C)		159.5 (C)		158.8 (C)
10		103.5 (C)		103.1 (C)		103.2 (C)		102.9 (C)
1'		109.0 (C)		108.1 (C)		122.2 (C)		121.8 (C)
2'		154.6 (C)		155.7 (C)	7.73 (1H, d, 2.1)	115.6 (CH)	7.69 (1H, d, 1.6)	115.6 (CH)
3'	6.54 (1H, d, 2.4)	103.3 (CH)	6.50 (1H, d, 2.4)	103.2 (CH)		145.2 (C)		145.1 (C)
4'		161.8 (C)		159.6 (C)		147.8 (C)		147.8 (C)
5'	7.75 (1H, d, 8.7)	106.9 (CH)	7.76 (1H, d, 8.7)	106.6 (CH)	6.91 (1H, d, 8.4)	115.6 (CH)	6.89 (1H, d, 8.4)	115.0 (CH)
6'	6.42 (1H, dd, 8.7, 2.4)	129.8 (CH)	6.44 (1H, dd, 8.7, 2.4)	129.7 (CH)	7.52 (1H, dd, 8.4, 2.1)	119.8 (CH)	7.56 (1H, dd, 8.4, 1.6)	120.0 (CH)
α1	7.41 (1H, d, 16.8)	130.2 (CH)			7.47 (1H, d, 16.8)	129.9 (CH)		
β1	7.54 (1H, d, 16.8)	118.2 (CH)			7.59 (1H, d, 16.8)	118.0 (CH)		
1''		138.3 (C)				138.3 (C)		
2'', 6''	7.52 (2H, d, 7.5)	125.8 (CH)				125.8 (CH)		
3'', 5''	7.40 (2H, d, 7.5)	128.8 (CH)				128.8 (CH)		
4''	7.26 (1H, t, 7.2)	127.2 (CH)				127.2 (CH)		
α2			7.36 (1H, d, 16.8)	130.4 (CH)			7.37 (1H, d, 16.8)	130.7 (CH)
β2			7.66 (1H, d, 16.8)	118.8 (CH)			7.66 (1H, d, 16.8)	118.6 (CH)
1'''				138.6 (C)				138.5 (C)
2''', 6'''			7.51 (2H, d, 7.5)	125.9 (CH)	7.54 (2H, d, 7.5)		7.52 (1H, d, 8.0)	125.9 (CH)
3''', 5'''			7.35 (2H, d, 7.5)	128.7 (CH)	7.38 (2H, d, 7.5)		7.36 (1H, d, 8.0)	128.8 (CH)
4'''			7.24 (1H, t, 7.2)	127.1 (CH)	7.26 (1H, t, 7.2)		7.25 (1H, t, 7.2)	127.2 (CH)
OH-5	13.36 (1H, br s)		14.28 (1H, s)		12.81 (1H, s)		13.69 (1H, s)	
OH-7	10.81 (1H, s)		10.79 (1H, s)		9.49 (1H, s)		11.34 (1H, s)	
OH-3					9.49 (1H, s)		9.60 (1H, s)	
OH-2'	10.81 (1H, s)		10.79 (1H, s)					
OH-3'					9.49 (1H, s)		9.46 (1H, s)	
OH-4'	10.81 (1H, s)		10.27 (1H, s)		9.49 (1H, s)		9.33 (1H, s)	

^a At 300 MHz.

^b At 75 MHz.

^c At 400 MHz.

^d At 100 MHz.

the formation of PhIP in roast beef patties. UPLC–MS analysis was used to detect the content of PhIP in roast beef patties before and after the addition of flavonoids. The content of PhIP was identified with corresponding yields of 2.60 ± 0.30 ng/g in control. As shown in Fig. 1, naringenin 0.2 mM can significantly ($p < 0.05$) inhibit PhIP formation, with an inhibition rate of 41.86%, norartocarpetin at 0.2 mM can also effectively inhibit PhIP formation, inhibition rate up to 25.16%. From the above results, the inhibition effects on PhIP formation of flavonoids were different and might be affected by their skeletons (for example, a double bond at 2 and 3 positions of C ring), the number and the position of hydroxyl group substituents attached on the flavonoid skeleton. In order to obtain the compounds with the best inhibitory effects on PhIP formation, it is necessary to further perform structure–activity relationship studies.

3.2. Identification of flavonoid–phenylacetaldehyde adducts in roast beef patties

The previous studies of Cheng et al. (2008, 2009) and Wong, Cheng, and Wang (2012) have revealed that naringenin, epigallocatechin gallate (EGCG), and pyridoxamine can inhibit PhIP formation via scavenging of phenylacetaldehyde and forming their adducts. In this study, six flavonoid–phenylacetaldehyde adducts were identified by UPLC–MS analysis and were further confirmed by their synthetic reference substances.

As for naringenin–phenylacetaldehyde adducts, two extracted molecular ion peaks (Fig. 2A1) at 373.1 (m/z [M–H][−]) (Fig. 2C1

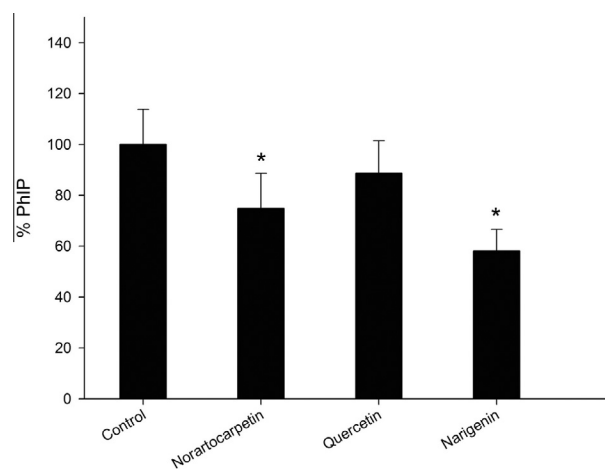


Fig. 1. The inhibitory effects of three flavonoids on the formation of PhIP in roast beef samples. $p < 0.05$ versus control.

and D1) were detected in negative ESI–MS, they belonged to the molecular ion peaks of NA1 and NA2, for which the molecular weight was 374, corresponding to the adducts between naringenin and phenylacetaldehyde followed by elimination of a water molecule; this is in agreement with a previous report (Cheng et al., 2008). Similar to naringenin, norartocarpetin reacted with phenylacetaldehyde and formed the adducts NARA1 and NARA2; this could be confirmed by detecting two molecular ion peaks

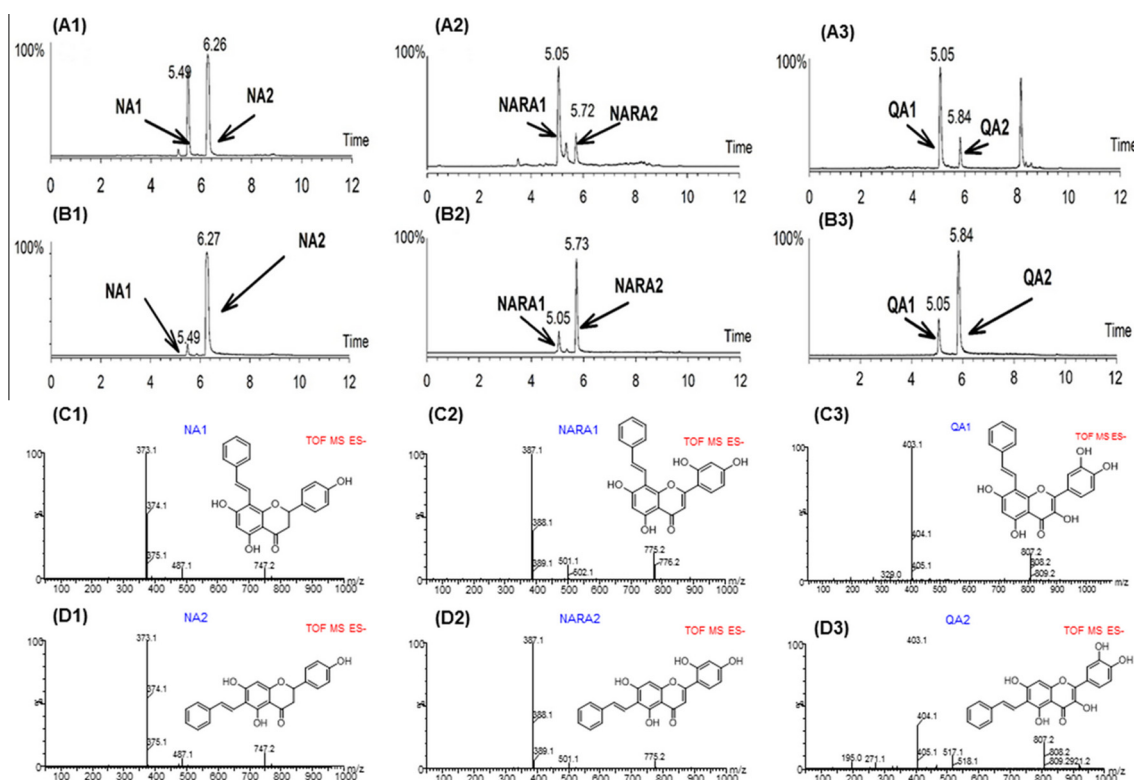


Fig. 2. Flavonoid–phenylacetaldehyde adducts in roast beef patties detected by UPLC–MS. Extracted ion chromatograms of flavonoid–phenylacetaldehyde adducts in roast beef samples (A) and pure synthetic reference substances (B), ESI–MS spectrum of flavonoid–phenylacetaldehyde adducts (C and D).

(Fig. 2A2) at 387.1 (m/z $[M-H]^-$) (Fig. 2C2 and D2) in negative ESI–MS with the molecular weight of 388, corresponding to the adducts between norartocarpetin and phenylacetaldehyde followed by elimination of a water molecule. In regard to quercetin–phenylacetaldehyde adducts, only one molecular ion peak (Fig. 2A3) at 403.1 (m/z $[M-H]^-$) (Fig. 2C3 and D3) in negative ESI–MS was found, which belonged to the adduct of QA1 and QA2, and its molecular weight was 404, corresponding to the adduct between quercetin and phenylacetaldehyde followed by elimination of a water molecule, suggesting that quercetin reacted with phenylacetaldehyde also forming an adduct. These adducts were further confirmed by their synthetic substances using UPLC–MS. It was found that beef samples treated with three flavonoids under heating contained analytes whose UPLC behaviour and MS spectral characteristics completely matched with those of the synthetic reference compounds (Fig. 2B1–B3). Six flavonoid–phenylacetaldehyde adducts formed from the reaction between three flavonoids and phenylacetaldehyde were detected by UPLC–MS and were further confirmed by their synthetic reference adducts. These results suggested that the inhibition mechanism of flavonoids on Phip formation was mainly *via* trapping its key intermediate, phenylacetaldehyde, consistent with previous studies (Cheng et al., 2008, 2009).

3.3. Synthesis, isolation, and characterisation of the structure of flavonoid–phenylacetaldehyde adducts

In order to further confirm the flavonoid–phenylacetaldehyde adducts and evaluate their biological activities, a slightly modified synthesis procedure was performed on the base of a previous study (Cheng et al., 2008). Six flavonoid–phenylacetaldehyde adducts were synthesised by the reaction between three flavonoids (naringenin, norartocarpetin, and quercetin) and phenylacetaldehyde.

The purified adducts were obtained through Sephadex LH-20 column chromatography. The structures of 8-*C*-(*E*-phenylethenyl)naringenin (NA1) and 6-*C*-(*E*-phenylethenyl)naringenin (NA2) were determined by 1H NMR, ^{13}C NMR (Table S1) spectroscopy, LC–MS data and comparison with the literature (Cheng et al., 2008), while the structures of 8-*C*-(*E*-phenylethenyl)norartocarpetin (NARA1), 6-*C*-(*E*-phenylethenyl)norartocarpetin (NARA2), and 8-*C*-(*E*-phenylethenyl)quercetin (QA1) and 6-*C*-(*E*-phenylethenyl)quercetin (QA2) were determined by 1H NMR, ^{13}C NMR (Table 1) spectroscopy, LC–MS data and on the basis of comparison with naringenin–phenylacetaldehyde adducts.

3.4. Effects of six adducts on the growth of liver cancer cell lines HepG2, SMMC-7721 and QGY-7703

Three different liver cancer cell lines (HepG2, SMMC-7721 and QGY-7703) were applied in the MTT assay to determine the effects of these adducts. After 24 h of treatment, NA1, NA2, NARA2, QA1, and QA2 showed moderate cytotoxic activity, with IC_{50} values ranging from 10 to 40 μM upon at least two of the liver cancer cell lines (Table 2), whereas NARA1 showed the strongest inhibitory effect on the growth of HepG2, SMMC-7721 and QGY-7703, with IC_{50} values of 7.06 ± 0.69 , 7.23 ± 0.15 and 7.69 ± 0.33 μM (Table 2). Under the current conditions, the inhibitory effects of NARA1 on these three liver cancer cell lines were more potent than those of the positive control, 5-fluorouracil (5-FU) ($IC_{50} > 100$ μM) (Table 2). Therefore, the effect of NARA1 deserved further investigation.

3.5. Effects of NARA1 on the caspase-dependent apoptosis upon liver cancer cell lines HepG2, SMMC-7721 and QGY-7703

Apoptosis is well known as the main outcome of anticancer chemotherapies, inducing cancer cell death with no inflammation

Table 2

Cytotoxic effects of three flavonoids and flavonoid–phenylacetaldehyde adducts against different liver cancer cell lines.

Compounds and adducts	Cancer cell lines $IC_{50} \pm SD^a$ (μM)		
	HepG2	SMMC-7721	QGY-7703
Naringenin	>40	>40	>40
NA1	25.20 \pm 1.00	18.18 \pm 0.85	14.06 \pm 0.83
NA2	14.79 \pm 0.77	22.49 \pm 0.47	10.34 \pm 0.91
Norartocarpetin	>40	>40	>40
NARA1	7.06 \pm 0.69	7.23 \pm 0.15	7.69 \pm 0.33
NARA2	34.67 \pm 0.59	30.32 \pm 0.42	39.97 \pm 0.51
Quercetin	22.16 \pm 0.63	>40	18.90 \pm 0.48
QA1	>40	>40	13.66 \pm 0.90
QA2	25.76 \pm 1.12	>40	17.70 \pm 0.49
5-FU ^b	>100	>100	>100

^a Values are means \pm SD ($n = 3$).

^b Positive control.

responses. It is characterised by several cellular and biochemical hallmarks, including membrane blebbing, cell shrinkage, nucleus condensation, and PARP cleavage. DAPI staining assay was applied to determine whether **NARA1** could induce apoptosis on HepG2, SMMC-7721 and QGY-7703 cancer cell lines. Fig. 3 showed that different degrees of apoptotic bodies were clearly observed after administration of the indicated concentration of **NARA1** at 12 and 24 h on HepG2, SMMC-7721 and QGY-7703 cell lines. The apoptotic bodies appeared increasing in a dose- and time-dependent manner in all these three cell lines (Fig. 3A). In addition, the cleaved-PARP was clearly exhibited after **NARA1** treatment for 24 h (Fig. 4). All these data demonstrated that **NARA1** obviously induced apoptosis in HepG2, SMMC-7721 and QGY-7703 cancer cell lines. To further determine whether the apoptosis is caspase-dependent, we evaluated the cell viability after pretreatment with

50 μM broad Z-VAD-fmk (pan-spectrum caspase inhibitor) 1 h before 24 h **NARA1** administration. Remarkable increases in cell number and improvement in cell morphology were found compared to **NARA1** alone (Fig. 3B). Meanwhile, the observations of the reduced cleaved-PARP after pretreatment of 50 μM Z-VAD-fmk and the dose-dependent decreased pro-caspase-9 were detected by western blot (Fig. 4), demonstrating the activation of caspase-related intrinsic apoptotic pathways.

3.6. Effects of NARA1 on G1 cell cycle arrest upon liver cancer cell lines HepG2, SMMC-7721 and QGY-7703

The MAPK and PI3K/AKT pathways are two of the main pathways to control cell survival. In particular, the MAPK signalling pathways are involved in affecting cell proliferation, differentiation, survival and migration, which include ERK, p38 and JNK MAPK pathways. All the MAPK pathways exhibit a complex function in cancer development. Activated ERK/p38 MAPK pathways in human cancers or mouse models have a dual role in tumorigenesis or in tumour suppression (Tong, Huang, & Pan, 2015; Wagner & Nebreda, 2009). Pharmacological inhibition of ERK activation attenuated pemetrexed-induced autophagy, enhanced HepG2 cell death and apoptosis (Tong et al., 2015). In accord with this report, the combination of PD98059 and **NARA1** induced more serious apoptosis of HepG2 (Fig. 4A). In HCC, higher JNK1 activation was correlated with a proliferation increase of tumour cells (Bubici & Papa, 2014). The present result showed more apoptotic cells after combination of **NARA1** with SP600125 in these three different HCC cell lines (Fig. 4A–C). In addition, we found the attenuation of apoptosis after combination of SB203580 with **NARA1**, demonstrating that **NARA1**-induced apoptosis in the HepG2 and QGY-7703 cell lines is p38 MAPK signalling-related (Fig. 4A and C). Therefore, the activation of ERK, p38 and JNK MAPK pathways,

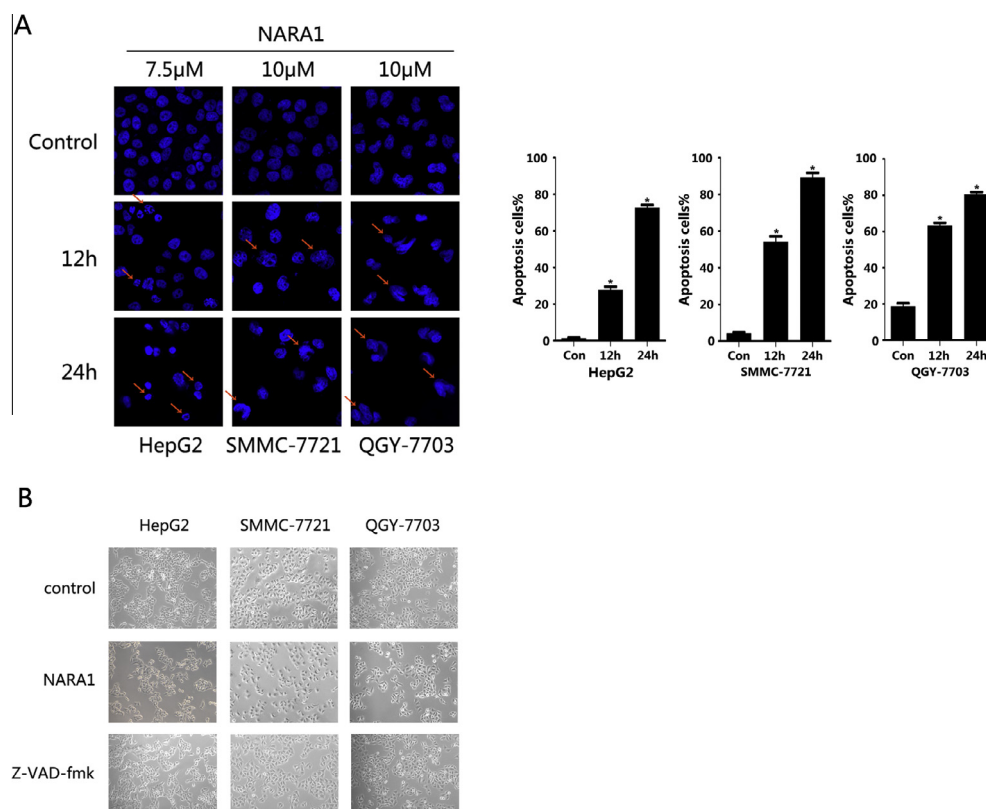


Fig. 3. **NARA1** induces apoptosis in HepG2, SMMC-7721, QGY-7703 cancer cell lines. After drug administration at indicated concentrations, the cells were stained by DAPI and visualised by fluorescence microscope at 12 and 24 h. Arrows show the apoptotic cells (A). Effects of **NARA1** on the apoptosis pathway in HepG2, SMMC-7721, QGY-7703 cells pretreated with 50 μM Z-VAD-fmk for 1 h. Results show the representative images of three independent experiments ($n = 3$) (B).

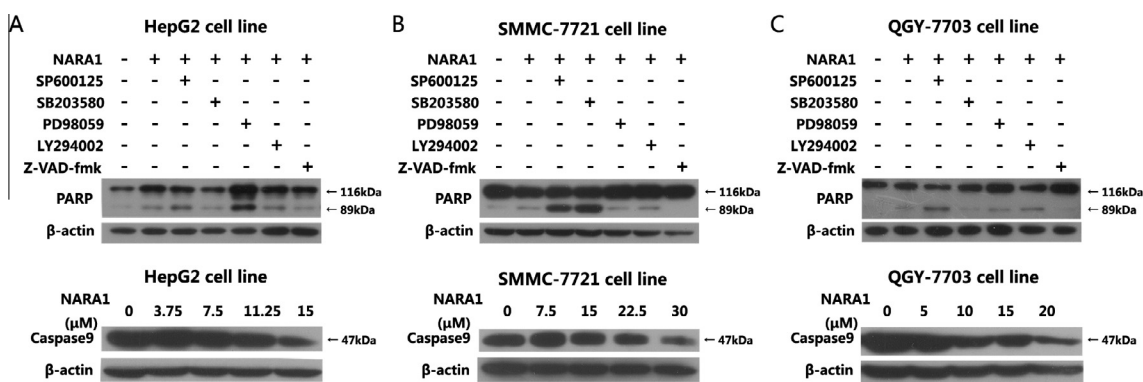


Fig. 4. Western blot analysis was used to evaluate PARP cleavage after drug administration for 24 h or pretreated with SP600125, SB203580, PD98059, LY294002 or Z-VAD-fmk for 1 h before **NARA1** administration, and the changes of caspase-9 after indicated concentration of **NARA1** for 24 h in HepG2 (A), SMMC-7721 (B), QGY-7703 (C) cancer cell lines. Results are representative of three independent experiments ($n = 3$).

leading to cell proliferation, differentiation, death and survival, depends on the cell type and the cell context. The detailed mechanism deserves further investigation.

4. Conclusions

Altogether, the results from this study demonstrated that some flavonoids could greatly reduce the content of PhIP in cooked beef meat, and their inhibition effects on PhIP formation were different and should be affected by the skeleton of the flavonoid and its substituent groups. Meanwhile, flavonoid–phenylacetaldehyde adducts were formed after flavonoids were added to inhibit PhIP formation in cooked beef meat. Further study showed that flavonoid–phenylacetaldehyde adducts exhibited cytotoxicity on some liver cancer cells, whereas their cytotoxicity depended on the structures of the flavonoids and the attached position of phenylacetaldehyde. More interesting, our findings revealed that 8-C-(*E*-phenylethenyl)norartocarpetin showed the strongest cytotoxicity toward different HCC cell lines, but the effects associated with MAPKs pathways were cell type-dependent. This finding is useful evidence that flavonoid adducts could be used to design new drugs to treat liver cancer.

Acknowledgements

This project was supported by the grant from the National Natural Science Foundation of China (No. 81202956), the National Basic Research Program of China (973 Program, 2012CB720801), the National Science Foundation of Jiangsu Province of China (BK20141110), and the Independent Research Program of State Key Laboratory of Food Science and Technology of China (SKLF-ZZA-201510).

Appendix A. Supplementary data

Supplementary data associated with this article can be found, in the online version, at <http://dx.doi.org/10.1016/j.foodchem.2015.11.104>.

References

Ahn, J., & Grun, I. U. (2005). Heterocyclic amines: 1. Kinetics of formation of polar and nonpolar heterocyclic amines as a function of time and temperature. *Journal of Food Science*, *70*, C173–C179.

Ambrosone, C. B., Abrams, S. M., Gorlewska-Roberts, K., & Kadlubar, F. F. (2007). Hair dye use, meat intake, and tobacco exposure and presence of carcinogen-DNA adducts in exfoliated breast ductal epithelial cells. *Archives of Biochemistry and Biophysics*, *464*, 169–175.

Bacon, J. R., Williamson, G., Garner, R. C., Lappin, G., Langouët, S., & Bao, Y. (2003). Sulforaphane and quercetin modulate PhIP-DNA adduct formation in human HepG2 cells and hepatocytes. *Carcinogenesis*, *24*, 1903–1911.

Bogen, K. T., Keating, G. A., Chan, J. M., Paine, L. J., Simms, E. L., Nelson, D. O., & Holly, E. A. (2007). Highly elevated PSA and dietary PhIP intake in a prospective clinic-based study among African Americans. *Prostate Cancer Prostatic Diseases*, *10*, 261–269.

Bubici, C., & Papa, S. (2014). JNK signaling in cancer: In need of new, smarter therapeutic targets. *British Journal of Pharmacology*, *171*, 24–37.

Busquets, R., Puignou, L., Galceran, M. T., & Skog, K. (2006). Effect of red wine marinades on the formation of heterocyclic amines in fried chicken breast. *Journal of Agricultural and Food Chemistry*, *54*, 8376–8384.

Cheng, K. W., Wong, C. C., Chao, J., Lo, C., Chen, F., Chu, I. K., ... Wang, M. (2009). Inhibition of mutagenic PhIP formation by epigallocatechin gallate via scavenging of phenylacetaldehyde. *Molecular Nutrition & Food Research*, *53*, 716–725.

Cheng, K. W., Wong, C. C., Cho, C. K., Chu, I. K., Sze, K. H., Lo, C., ... Wang, M. (2008). Trapping of phenylacetaldehyde as a key mechanism responsible for naringenin's inhibitory activity in mutagenic 2-amino-1-methyl-6-phenylimidazo[4,5-b]pyridine formation. *Chemical Research in Toxicology*, *21*, 2026–2034.

Chu, F. L., & Yaylayan, V. (2008). Model studies on the oxygen-induced formation of benzaldehyde from phenylacetaldehyde using pyrolysis GC-MS and FTIR. *Journal of Agricultural and Food Chemistry*, *56*, 10697–10704.

Freedman, N. D., Cross, A. J., McGlynn, K. A., Abnet, C. C., Park, Y., Hollenbeck, A. R., ... Sinha, R. (2010). Association of meat and fat intake with liver disease and hepatocellular carcinoma in the NIH-AARP cohort. *Journal of the National Cancer Institute*, *102*, 1354–1365.

Li, H., Zhu, F., Chen, H., Cheng, K. W., Zykova, T., Oi, N., ... Dong, Z. (2014). 6-C-(*E*-phenylethenyl)naringenin suppresses colorectal cancer growth by inhibiting cyclooxygenase-1. *Cancer Research*, *74*, 243–252.

Malfatti, M. A., Dingley, K. H., Nowell-Kadlubar, S., Ubick, E. A., Mulakken, N., Nelson, D., ... Turteltaub, K. W. (2006). The urinary metabolite profile of the dietary carcinogen 2-amino-1-methyl-6-phenylimidazo[4,5-b]pyridine is predictive of colon DNA adducts after a low-dose exposure in humans. *Cancer Research*, *66*, 10541–10547.

Messner, C., & Murkovic, M. (2004). Evaluation of a new model system for studying the formation of heterocyclic amines. *Journal of Chromatography B*, *802*, 19–26.

Murkovic, M., Steinberger, D., & Pfannhauser, W. (1998). Antioxidant spices reduce the formation of heterocyclic amines in fried meat. *Zeitschrift für Lebensmittel-Untersuchung und Forschung A*, *207*, 477–480.

Murkovic, M., Weber, H. J., Geiszler, S., Fröhlich, K., & Pfannhauser, W. (1999). Formation of the food associated carcinogen 2-amino-1-methyl-6-phenylimidazo[4,5-b]pyridine (PhIP) in model systems. *Food Chemistry*, *65*, 233–237.

Salazar, R., Arambula-Villa, G., Hidalgo, F. J., & Zamora, R. (2014). Structural characteristics that determine the inhibitory role of phenolic compounds on 2-amino-1-methyl-6-phenylimidazo[4,5-b]pyridine (PhIP) formation. *Food Chemistry*, *151*, 480–486.

Shin, A., Shrubsole, M. J., Ness, R. M., Wu, H., Sinha, R., Smalley, W. E., ... Zheng, W. (2007). Meat and meat-mutagen intake, doneness preference and the risk of colorectal polyps: The tennessee colorectal polyp study. *International Journal of Cancer*, *121*, 136–142.

Sinha, R., Gustafson, D. R., Kulldorff, M., Wen, W. Q., Cerhan, J. R., & Zheng, W. (2000). 2-Amino-1-methyl-6-phenylimidazo[4,5-b]pyridine, a carcinogen in high-temperature-cooked meat, and breast cancer risk. *Journal of the National Cancer Institute*, *92*, 1352–1354.

Sinha, R., Peters, U., Cross, A. J., Kulldorff, M., Weissfeld, J. L., Pinsky, P. F., ... Hayes, R. B. (2005). Meat, meat cooking methods and preservation, and risk for colorectal adenoma. *Cancer Research*, *65*, 8034–8041.

Skog, K. I., Johansson, M. A., & Jagerstad, M. I. (1998). Carcinogenic heterocyclic amines in model systems and cooked foods: A review on formation, occurrence and intake. *Food and Chemical Toxicology*, *36*, 879–896.

- Skog, K., Steineck, G., Augustsson, K., & Margaretha, J. (1995). Effect of cooking temperature on the formation of heterocyclic amines in fried meat products and pan residues. *Carcinogenesis*, *16*, 861–867.
- Tang, D., Liu, J. J., Rundle, A., Neslund-Dudas, C., Saveria, A. T., Bock, C. H., ... Rybicki, B. A. (2007). Grilled meat consumption and PhIP-DNA adducts in prostate carcinogenesis. *Cancer Epidemiology, Biomarkers & Prevention*, *16*, 803–808.
- Tieman, D. M., Loucas, H. M., Kim, J. Y., Clark, D. G., & Klee, H. J. (2007). Tomato phenylacetaldehyde reductases catalyze the last step in the synthesis of the aroma volatile 2-phenylethanol. *Phytochemistry*, *68*, 2660–2669.
- Tong, Y., Huang, H., & Pan, H. (2015). Inhibition of MEK/ERK activation attenuates autophagy and potentiates pemetrexed-induced activity against HepG2 hepatocellular carcinoma cells. *Biochemical and Biophysical Research Communications*, *456*, 86–91.
- Wagner, E. F., & Nebreda, A. (2009). Signal integration by JNK and P38 MSPK pathways in cancer development. *Nature Reviews Cancer*, *9*, 537–549.
- Wakabayashi, K., Nagao, M., Esumi, H., & Sugimura, T. (1992). Food-derived mutagens and carcinogens. *Cancer Research*, *52*(Suppl.), 2092–2098.
- Warzecha, L., Janoszka, B., Blaszczyk, U., Strozyk, M., Bodzek, D., & Dobosz, C. (2004). Determination of heterocyclic aromatic amines (HAs) content in samples of household-prepared meat dishes. *Journal of Chromatography B*, *802*, 95–106.
- Wong, D., Cheng, K. W., & Wang, M. (2012). Inhibition of heterocyclic amine formation by water-soluble vitamins in Maillard reaction model systems and beef patties. *Food Chemistry*, *133*, 760–766.
- Yan, Y., Zeng, M., Zheng, Z. P., He, Z., Tao, G., Zhang, S., ... Chen, J. (2014). Simultaneous analysis of PhIP, 4'-OH-PhIP and their precursors using UHPLC-MS/MS. *Journal of Agricultural and Food Chemistry*, *62*, 11628–11636.
- Zamora, R., Alcon, E., & Hidalgo, F. J. (2014). Ammonia and formaldehyde participate in the formation of 2-amino-1-methyl-6-phenylimidazo[4,5-b]pyridine (PhIP) in addition to creati(ni)ne and phenylacetaldehyde. *Food Chemistry*, *155*, 74–80.
- Zheng, Z. P., Xu, Y., Qin, C., Zhang, S., Gu, X., Lin, Y., ... Chen, J. (2014). Characterization of antiproliferative activity constituents from *Artocarpus heterophyllus*. *Journal of Agricultural and Food Chemistry*, *62*, 5519–5527.